Intelligent Transportation Infrastructure, 2024, liae001
https://doi.org/10.1093/iti/liae001
Research Article

Advancing a major US airline's practice in flight-level checked baggage prediction

Shijie Chen[1], Chiwoo Park[1], Qianwen Guo[2], Yanshuo Sun[1,*]

[1]Department of Industrial and Manufacturing Engineering, FAMU-FSU College of Engineering, Florida State University, 2525 Pottsdamer Street, Tallahassee, FL, 32312, USA
[2]Department of Civil and Environmental Engineering, FAMU-FSU College of Engineering, Florida State University, 2525 Pottsdamer Street, Tallahassee, FL, 32312, USA

[*]Corresponding author: Email: y.sun@eng.famu.fsu.edu

In this paper, we aim to address a relevant estimation problem that aviation professionals encounter in their daily operations. Specifically, aircraft load planners require information on the expected number of checked bags for a flight several hours prior to its scheduled departure to properly palletize and load the aircraft. However, the checked baggage prediction problem has not been sufficiently studied in the literature, particularly at the flight level. Existing prediction approaches have not properly accounted for the different impacts of overestimating and underestimating checked baggage volumes on airline operations. Therefore, we propose a custom loss function, in the form of a piecewise quadratic function, which aligns with airline operations practice and utilizes machine learning algorithms to optimize checked baggage predictions incorporating the new loss function. We consider multiple linear regression, LightGBM, and XGBoost, as supervised learning algorithms. We apply our proposed methods to baggage data from a major airline and additional data from various US government agencies. We compare the performance of the three customized supervised learning algorithms. We find that the two gradient boosting methods (i.e., LightGBM and XGBoost) yield higher accuracy than the multiple linear regression; XGBoost outperforms LightGBM while LightGBM requires much less training time than XGBoost. We also investigate the performance of XGBoost on samples from different categories and provide insights for selecting an appropriate prediction algorithm to improve baggage prediction practices. Our modeling framework can be adapted to address other prediction challenges in aviation, such as predicting the number of standby passengers or no-shows.

Keywords: aviation; airline operations; checked baggage; supervised learning; custom loss function

1. Introduction

The air transportation system is a complex network of internal and external entities that interact with one another in a variety of ways. For example, passengers can choose from multiple flights operated by competing airlines, airlines plan and schedule their flights to minimize operating costs, and air traffic controllers ensure safety and minimize delays for flights sharing the airspace. The air transportation system is also affected by external factors such as weather and socio-economic systems (Jardines et al., 2021), which contribute to the generation of large and intricate datasets. By analyzing these datasets effectively, there is great potential for the aviation sector to undergo significant transformation. The Next Generation Air Transportation System (NextGen) is an initiative led by the National Aeronautics and Space Administration (NASA) and Federal Aviation Administration (FAA) to use advanced data mining tools to identify safety vulnerabilities across various types of data (NASA 2007). Outside of air traffic management (ATM), airlines have also been known for improving revenues by tailoring their services and products to various customer segments based on analyses of their very rich passenger booking data (Sun et al., 2018). This paper aims to explore how advanced machine learning algorithms and large-volume operational data can revolutionize conventional practices in airline operations, with a particular focus on the flight-level checked baggage prediction problem, to be defined and analyzed next.

A few hours (e.g., three to four hours) before the departure of a passenger flight, load planners need to decide what shipments booked on this flight can be selected for loading or off-loading, how selected shipments can be packed into unit load devices (ULDs) or palletized, and how ULDs or pallets can be assigned to different positions on the aircraft (Brandt & Nickel 2019). Those loading decisions depend on how much checked baggage to anticipate, whose exact amount only becomes available shortly (such as 45 minutes) before the scheduled departure. Thus, the expected number of checked bags must be estimated in advance, to facilitate the aircraft load planning process where various weight and balance limits should be enforced. For instance, the maximum cargo (including checked baggage) to carry should be jointly determined with fuel load subject to the takeoff weight limit (FAA 2016). From the perspective of balance control, flight safety concerns may arise from baggage issues. A shift in the longitudinal center of gravity, caused by improperly loaded baggage, may result in unstable aircraft conditions or difficulty in controlling the aircraft (FAA 2023). In addition, loading checked bags can be time-consuming and labor-intensive. Having relatively accurate checked baggage information would allow an airline to

Received: December 17, 2023. **Revised:** February 14, 2024. **Accepted:** February 27, 2024

allocate appropriate human power to load checked bags on to an airplane (BEONTRA 2022). In case of an unusually large number of bags, the baggage loading process would be prolonged, thus likely delaying a flight. While a good estimation of checked baggage is highly desirable, it is difficult to achieve such a prediction because the amount of checked baggage usually fluctuates substantially, due to the influence of various factors, such as passenger trip purposes and travel seasons.

A detailed literature review (to be presented in Section 2) indicates that only a few studies have focused on the checked baggage prediction problem and each of them has various shortcomings. For instance, non-time-series data cannot be easily incorporated into a time-series forecasting model for baggage prediction, as in Ma et al., (2021). The primary shortcoming of the existing literature is that the consequences of over-prediction and under-prediction are treated equally, contrary to aviation practice. Modeling the asymmetric effect is important in the context of baggage prediction, as the cost of not having sufficient space to accommodate checked baggage is much higher than having a partially filled checked baggage compartment.

In this study, we analyzed a checked baggage dataset consisting of nearly one million samples owned by a major US airline. The primary dataset was enriched by including additional features, such as the population of a city and passenger enplanements of an airport. Next, we performed necessary data cleaning and feature processing to avoid the negative impact of data irregularities on the subsequent analyses and predictions. We introduced three prediction methods: linear regression and two advanced supervised learning algorithms (i.e., LightGBM and XGBoost). We further customized these by designing and incorporating an asymmetric loss function. Some findings from the experiments are highlighted as follows: (1) LightGBM and XGBoost can achieve a much better predictive performance than linear regression regardless of whether the asymmetric loss function is considered or not, while XGBboost slightly outperforms LightGBM; (2)LightGBM is significantly more efficient than XGBoost; (3) the predictive performance of XGBoost is not uniform over destination airports or fleet types due to uneven training data coverage.

To the best of our knowledge, this is the first flight-level checked baggage prediction study considering an asymmetric loss function. This study also demonstrates the great potential of state-of-the-art machine learning algorithms in modernizing some conventional practices in airline operations with large-scale real-world data.

The rest of this paper is organized as follows. Section 2 briefly reviews some machine learning applications in air transportation. We next describe in Section 3 how exploratory analyses of the datasets are conducted along with data cleaning and feature engineering. Then, in Section 4, multiple prediction methods of various complexities are introduced and the asymmetric loss function is presented. Experiments are conducted and major results are reported in Section 5. A discussion of how to choose an appropriate baggage prediction algorithm is presented in Section 6. Lastly, concluding remarks and future research directions are given in Section 7.

2. Literature review

We divide related machine learning applications in air transportation into two broad categories: flight-related and payload-related. In the first group, we mainly review those predictive studies on aircraft trajectory and flight delay; in the second group, we focus on those studies on passenger, cargo, and checked baggage predictions.

2.1 Flight-related problems

2.1.1 *Aircraft trajectory prediction*

In traditional ATM, controllers only need to know the current location of aircraft, while under the new trajectory-based operations (TBO) paradigm, controllers require information on the future location of aircraft as well (Mondoloni & Rozen 2020). This is where four-dimensional (4D) trajectory prediction (TP) is needed (Wang et al., 2020; Wu et al., 2022). This involves predicting an aircraft's longitude, latitude, altitude, and time, and is crucial for improving air traffic safety and ATM efficiency under TBO. This is because an aircraft's actual trajectory can deviate from its planned route due to various factors such as congestion and weather conditions. Trajectories can be predicted either in the short term (in-flight) or long term (pre-flight). Two representative studies are reviewed next.

In a short-term predictive study, Gallego et al., (2019) proposed a measure of probabilistic interdependence for pairs of aircraft, which they used as a feature to predict the vertical profiles of aircraft trajectories during the descent phase of flight. Their study employed data from the Barcelona Air Traffic Control Center in Spain and demonstrated the usefulness of their neural network methods. The researchers concluded that incorporating the proposed interdependence measure enhanced the accuracy of trajectory prediction. In contrast, Wu et al., (2022) focused on predicting the 4D trajectory of an aircraft prior to takeoff using historical trajectory data. To achieve this, they converted historical time-series data into images and used various types of generative adversarial networks (GANs) to generate new images, which were then transformed into time-series data or flight trajectories. The study used data from flights between Beijing and Chengdu in China and compared different GAN variants based on training time, prediction time, and prediction accuracy. The researchers found that the one-dimensional convolution variant of GAN produced the best results.

2.1.2 *Flight delay*

The issue of flight delays has a significant impact on airline operations and customer satisfaction, leading many researchers to focus on predicting flight delays using machine learning. For example, Khan et al., (2021) observed that current flight delay classification systems use multiple threshold prediction classifiers running in parallel, which can lead to conflicting results and ambiguity. Instead, they proposed a sequential approach to predicting whether flight delays exceed certain thresholds by considering only part of the data. They demonstrated their prediction algorithms with a case study of an airline based in Hong Kong. In contrast, Rodríguez-Sanz et al., (2019) used a Bayesian network approach to predict delays for the arrival systems of an airport. They also conducted a reliability analysis using a Markov chain approach to evaluate the system's reliability. Their model can adaptively capture the stochastic characteristics of arrival processes. As it is beyond the scope of this study to further review those flight-related machine learning studies, interested readers are directed to Chung et al., (2020).

2.2 Payload-related problems

2.2.1 *Passengers and air cargo*

Passengers account for the majority of payload on commercial flights. Passenger demand predictions have been conducted at different levels, such as the national or airport level.

Xu et al., (2019) combined seasonal autoregressive integrated moving average (SARIMA) and support vector regression (SVR) for the prediction of several aviation metrics for China's aviation industry, such as domestic and international passenger miles. They used 133 observations between February 2005 and February 2016 to predict values from March 2016 to February 2018. While such predictions at a national level are useful for strategic planning purposes, other researchers have focused on operational problems at a lower level. For instance, to dynamically optimize the configurations of airport security screening lanes, Hanumantha et al., (2020) proposed an ensemble forecasting model, which was tested in a case study of Phoenix Sky Harbor Airport.

It is also very common for passenger flights to carry air cargo, which is organized using pallets or ULDs that are loaded into the belly of the fuselage under the passenger compartment. Such cargo space is shared by air cargo and checked baggage, while the latter has priority over the former. This implies that the available belly space for air cargo is uncertain. Therefore, Tseremoglou et al., (2022) used long short-term memory networks (LSTMs) to predict available cargo space. They then solved a real-time booking acceptance problem with the predicted values as inputs. Their experiments indicated that their proposed method can significantly increase loaded volume while decreasing unplanned offloading. A comprehensive review of the application of machine learning in air cargo management can be found in Barua et al., (2020).

While predicting cargo and passenger demand seems similar, the information provided by cargo tracking and passenger service systems could be quite different, implying that models for passengers and air cargo are not immediately transferable. Gender, age, and travel purpose are examples of common passenger characteristics that do not apply to cargo predictions.

2.2.2 *Checked baggage*

As the most relevant ones to this study, a few papers tried to predict the amount of checked baggage. Accurate prediction of checked baggage is fundamental for reasonable resource allocation to prevent the overloading of the baggage handling system (Ma et al., 2021) and to allocate staff resources (BEONTRA 2022). A SARIMA model was adopted by Ma et al., (2021) for checked baggage prediction at the airport level. Based on the historical baggage volume covering eight weeks, the demand for the subsequent three days was predicted. They quantified the predictive ability with some metrics but no alternative models were involved for benchmarking purposes. Mikram et al., (2020) also adopted the ARIMA model to forecast the baggage volume and found that the Box–Jenkins approach and exponential smoothing methods can improve the accuracy. One shortcoming of these time-series models is that they rely on time-series data only, which implies a lot of available passenger-related characteristics cannot be incorporated. In addition, those predictions are intended to be at the airport level, rather than the flight level.

Cheng et al., (2014) forecast the baggage volume for each flight from an international terminal using a back propagation neural network and multiple linear regression (MLR). Numerical experiments on three datasets of various sizes were conducted. Only five features were involved: passenger count, flight date, flight type, departure time, and flight duration. This study had a quite limited sample size. In predicting the baggage amount for a single flight, only 29 samples were used, among which 21 were for training and 8 were for testing. The entire dataset covering all flights had 3,040 samples. Given the limited number of features and sample size, the resulting R^2 is also quite low (i.e., slightly over 0.5).

The identification of mishandled bags was studied by van Leeuwen et al., (2020) using a Gradient Boosting machine, which was not reviewed in detail due to its low relevance.

2.3 Summary

The large amount of data generated in the aviation industry has led to extensive developments of machine learning algorithms for aviation transportation management (Xu et al., 2024). A good variety of aviation problems have been studied with machine learning (Chung et al., 2020). However, only a few studies were for predicting the amount of checked baggage. A shortcoming in the time-series models for checked baggage prediction is that the impact of many non-time-series data on passenger baggage volume cannot be incorporated. More importantly, none of those studies has explored an asymmetric loss function in predictive analyses. This paper is distinguished from those studies by presenting a flight-level checked baggage prediction method based on the customization of advanced machine learning algorithms. Another strength of the paper lies in the large-scale and multi-source datasets covering a whole country being analyzed in this study.

3. Data

3.1 Data sources and overview

The flight baggage dataset used in this study was obtained from a major US airline, referred to as Airline λ for confidentiality purposes due to the non-disclosure agreement. The dataset consisted of 926,395 domestic flights operated by the airline in 2019, predating the COVID-19 pandemic. Each row in the dataset represented a flight on a specific day, with operational details and aggregated passenger counts being available. The dataset consisted of 22 features related to flights, including flight number, departure and arrival date and time, origin and destination cities, aircraft type, leg distance, and the total number of onboard passengers. Additionally, there were 27 other features related to passenger characteristics, such as payment type, presence of a child or infant, booking method, and cabin class. Airline λ also categorized their passengers based on their loyalty status and predicted travel purposes by other undisclosed algorithms. All those passenger-related features combined presented valuable insights into understanding who those customers were, why they traveled, and how they checked bags. The dataset contained a single target variable, which was the number of checked bags on each flight.

While the baggage dataset from Airline λ was essential, additional data were obtained to enhance the predictive performance of machine learning algorithms. This was because the baggage dataset did not have key information about airports, cities, and air travel trends over time. For instance, the baggage dataset itself did not provide any information on how the population of Houston, Texas compared with that of Omaha, Nebraska; it did not tell how the Reagan National Airport's enplanements differed from the Dulles International Airport serving the same metropolitan area; it did not properly reflect the difference between Thanksgiving travels and New Year travels. Therefore, the following new features were added: city population from US Census Bureau (2021), annual enplanements by airports provided by FAA (2022), and the Transportation Security Administration (TSA) checkpoint travel numbers (TSA 2022). Figure 1 shows the ten busiest airports in 2021 by enplanement as well as the population of the city served

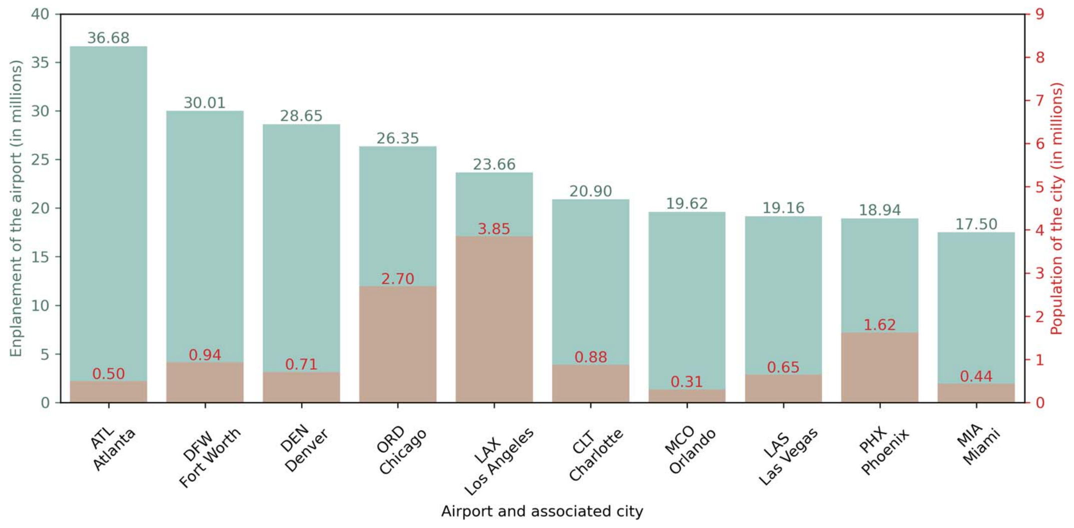

Figure 1 Top 10 busiest airports in USA in 2021 by enplanement.

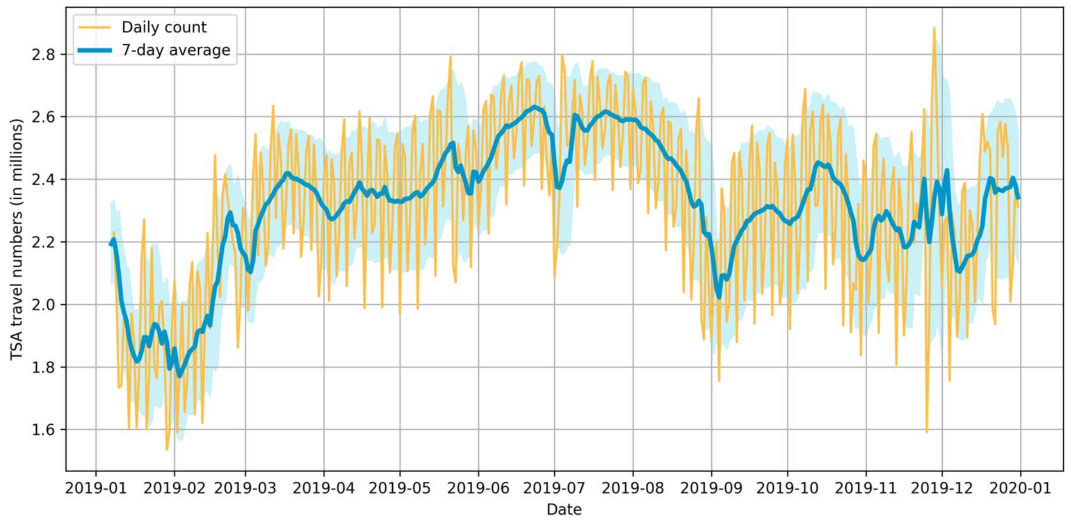

Figure 2 TSA checkpoint travel numbers in 2019.

by an airport. By enplanement, Atlanta Airport was followed by the Dallas and Denver airports. As no enplanement data were found for 2019, and to avoid considering the disruptions of the COVID-19 pandemic in 2020, the 2021 data were used instead. For the TSA daily count, historical data were found for 2019 and thus used. Figure 2 shows the TSA checkpoint travel numbers in 2019, displaying the air travel peaks in summer months, especially July and August, as well as off-peaks in February and September.

3.2 Data cleaning

According to Airline λ, the baggage dataset was real and unaltered. Although we did not find any missing values or duplicate records, some irregularities in the data were identified. Therefore, we used the following procedure to clean the baggage dataset. First, any rows with negative passenger counts were dropped. Second, if the aggregated passenger count over different categories exceeded the total count, relevant data were dropped. For instance, if the number of local and connecting passengers exceeded the total number of onboard passengers, the corresponding sample was removed. Similarly, the number of passengers in the main cabin cannot be greater than the total passenger count. Third, if the passenger and bag counts were conflicting, relevant data were removed. For instance, certain flights had a few—even zero—passengers while carrying over a hundred checked bags. If either the passenger or bag count was lower than ten, we removed such flights as outliers. After data cleaning, 722,556 records remained.

3.3 Data explorations

We next conducted several exploratory analyses to illustrate some important relations in the baggage dataset, which would have been hidden otherwise. Figure 3 shows how the target variable varies with two passenger-related features, namely the number of paying passengers and the number of main cabin passengers, as well as the histograms for those two features. In Fig. 3, the solid line represents the average bag count while the standard deviation of bag count is visualized by the buffer zone along the solid line. Those two solid lines seem very similar because of a high correlation between those two corresponding features. The majority of passengers pay for their travels, thus classified as paying passengers, and opt for the main cabin, thus classified as the main cabin passengers. While the ratio of revenue passengers to main cabin passengers varies, the average ratio is 0.9. It is also evident that as the number of passengers grows, the number of bags grows in general, especially before the

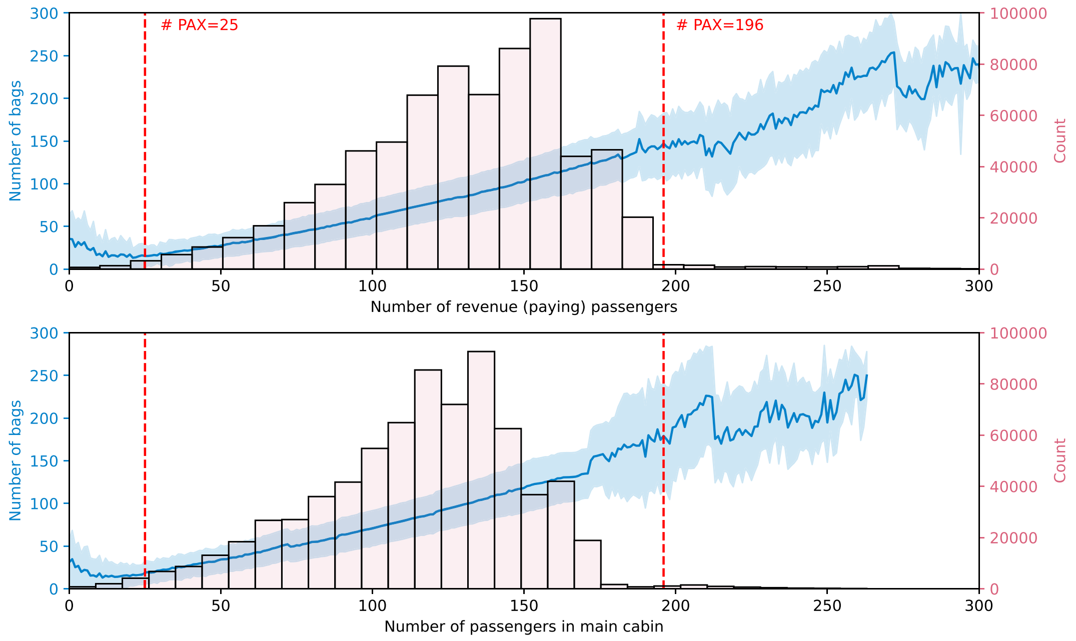

Figure 3 Bag count versus passenger count.

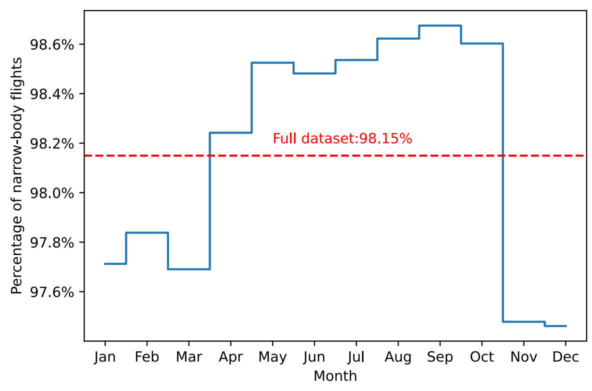

Figure 4 Percentage of flights using narrow-body aircraft over months.

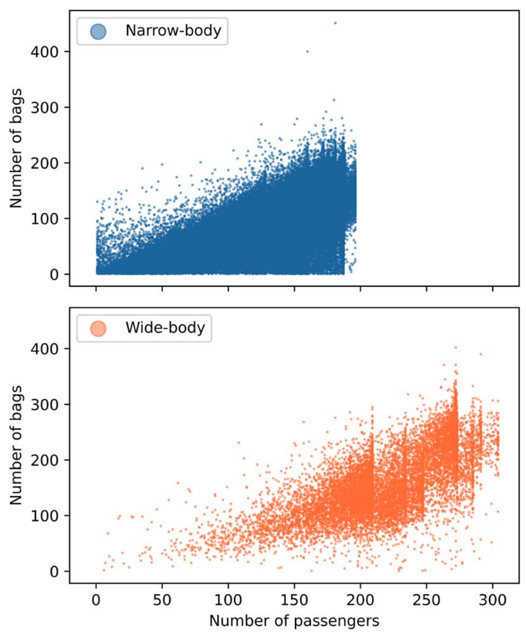

Figure 5 Number of bags by aircraft type.

number of revenue passengers hits 196. When there are more than 196 passengers on a flight, the relation between the bag and passenger counts is no longer smooth and the standard deviation also increases. The cutoff line represents the capacity of the largest narrow-body airplane used by the airline. Wide-body aircraft are capable of carrying more passengers than 196, while they are used for only 1.85 per cent of all the flights in the dataset, as shown in Fig. 4. The two histograms in Fig. 3 also indicate very few observations for wide-body aircraft. Given the limited sample size for wide-body aircraft, the bag–passenger relation is not characterized adequately by the current data. It is also notable that when the number of paying passengers is within 10, the bag count is nearly 50, implying an unusually large bag-to-passenger ratio.

Figure 5 indicates that wide-body aircraft carry significantly more checked bags as expected. Figure 6 presents the distribution of load factor, i.e., the total number of passengers divided by the aircraft capacity, which shows that in most cases, aircraft are nearly fully loaded.

We next explore how the counts of bags and passengers vary over time at different granularity levels (i.e., month, day of the week, and hour of the day). The way in which the bag count varies over months is very similar to the national air travel trend shown in Fig. 2. From Fig. 7, we observe more bags in summer months, such as June and July, while fewer bags are observed in September and October. In December, the bag count is the highest. This could be partially affected by school terms. For example, there might be more family travels for recreational purposes over the summer and winter breaks, contributing to the surges in bag. Figure 7 further shows that there are more checked bags on Saturday and Sunday flights and fewer on Wednesday and Thursday. As Airline λ did not operate any flights around 3 a.m. and 4 a.m., there is a gap in how the bag count varies with the hour of the day in Fig. 7. Flights carried fewer bags around midday and more bags close to midnight. This pattern may reflect a combination of operational scheduling by airlines and passenger preferences, with late-night flights possibly accommodating more long-haul or international travelers who tend to check in more baggage. Additionally, the

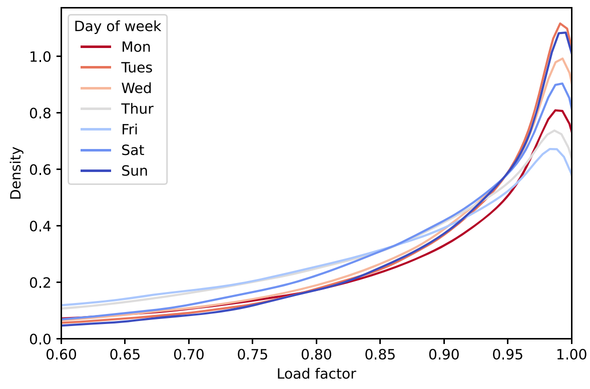

Figure 6 Density distribution for load factor over days of the week.

trend of increased baggage volumes close to midnight could be influenced by passengers choosing late-night flights for economic reasons or personal scheduling needs.

Figure 8 shows how passengers booked their tickets over time, for an example flight from a major hub (pseudonymized as Hub1) of Airline λ to New York City and a selected aircraft type Boeing 737. Approximately, 30 per cent of passengers booked their tickets one month in advance, and 65 per cent of passengers booked at least one week in advance. At the time of departure, 83.2 per cent of tickets were sold, which was close to the average load factor shown in Fig. 6.

Collinearity refers to a linear relationship between two or more predictor variables. This issue would become a concern in some regression models as the significance level of both variables will dramatically decrease and the estimated coefficients of the predictors are unstable (Wold et al., 1984). This issue was detected in the baggage dataset because the number of leisure passengers was presented twice. The first estimate was likely to have been obtained from the booking data while the second estimate was obtained with an 'improved' classification algorithm used by Airline λ. The two estimates were highly correlated, with a Pearson's correlation coefficient of 0.97. Therefore, one of the two variables was removed. Similarly, one variable related to business travelers was dropped.

3.4 Feature encoding

The baggage dataset consisted of many categorical variables, because quite a few time- and location-related features were involved, such as month, hour, day of the week, and airport code. If one-hot encoding was directly employed for all those categorical features, the number of additional dummy variables would be significant, especially when a categorical variable has many levels. For instance, when we examine the origin airport as a categorical variable, if there are 100 airports, the same number of dummy variables is needed with one variable corresponding to one airport. To avoid introducing too many additional features, we combined some levels for selected categorical features as shown in Table 1, mainly based on the data explorations described earlier. Hubs 1, 2, and 3 represent the three busiest hubs in the dataset, measured by the number of flights. Similarly, the encoding for the 'hour' feature into specific groups is informed by our analysis of operational patterns and baggage volume trends at airports. Specifically, we observed a consistent increase in baggage volumes during the hours of 0, 1, 2, and 23, as shown in Fig. 7(c). To protect the confidential and proprietary information of Airline λ, specific names of those hubs are not revealed, while this anonymization does not hurt the rigor and usefulness of this analysis.

Table 1. Grouping for categorical variables.

Categorical feature	Level grouping
Origin hub	[Hub1], [Hub2], [Hub3], [Others]
Destination hub	[Hub1], [Hub2], [Hub3], [Others]
Aircraft type	[330, 767, 777, 787], [Others]
Day of the week	[Wednesday, Thursday], [Monday, Sunday], [Others]
Hour	[0, 1, 2, 23], [Others]
Month	[9, 10, 11], [6, 7], [12], [Others]

Appendix A lists all features considered in the following predictive analyses. Specifically, 22 features are flight-related, 27 are related to passengers, and five are supplementary.

4. Methodology

In this section, we describe three machine learning algorithms to predict the checked baggage volume y given attributes $\mathbf{x}$, namely all features listed in Appendix A. Section 4.1 will describe the basic modeling propositions. Sections 4.2–4.4 will describe three predictive algorithms.

4.1 Basic modeling propositions

In machine learning, an unknown prediction function $f(\mathbf{x})$ that relates $\mathbf{x}$ and y is identified, using its N noisy observations,

$$y_i = f(\mathbf{x}_i) + \epsilon_i, i = 1, \dots, N, \tag{1}$$

where y_i and $\mathbf{x_i}$ are the dependent and explanatory variable values for the ith observation, respectively, ϵ_i is independent noise with a mean of zero and variance of σ^2, and N is the sample size. For $f(\mathbf{x})$, we consider MLR as the baseline benchmark, which is described in Section 4.2. We next consider two gradient boosting methods in Sections 4.3 and 4.4. We seek to find the best model $\hat{f}(\mathbf{x})$ that minimizes the training error:

$$J(\hat{f}) = \sum_{i=1}^{N} \ell(\hat{f}(\mathbf{x}_i), y_i). \tag{2}$$

Here, $\ell(\hat{f}(\mathbf{x}_i), y_i)$ is a loss function that quantifies the cost of making the prediction $\hat{f}(\mathbf{x}_i)$, which can be abbreviated as $\hat{y}_i$, when y_i is the actual value.

As for the loss function $\ell(\cdot)$, we consider the business costs related to the prediction inaccuracy. In airline operations, the business cost of underestimating checked bags is significantly higher than the cost of overestimation. In the case of underestimation, insufficient human power is allocated for loading checked bags, thus resulting in possible departure delays. Or there might not be enough storage room for checked bags on the departing airplane, which means customers may spend additional time waiting for their checked bags to arrive on another flight. Delayed bags may need to be shipped to customers' homes at a high cost. In the case of overestimation, the cargo compartment is partially filled, which incurs some opportunity cost, because some cargo shipments should have been loaded if an accurate count of checked bags has been estimated. To properly consider this cost asymmetry, we design the following piecewise quadratic loss function:

$$\ell(\hat{f}(\mathbf{x}_i), y_i) = \frac{c_o}{2}(\hat{y}_i - y_i)_+^2 + \frac{c_u}{2}(y_i - \hat{y}_i)_+^2. \tag{3}$$

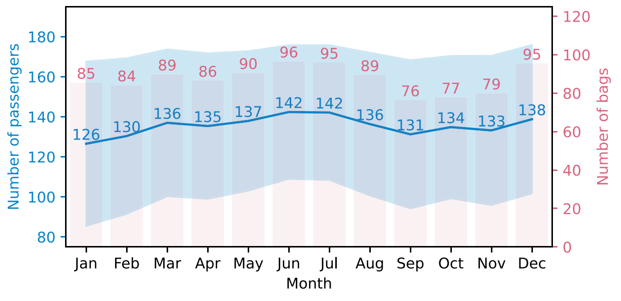

(a) Number of bags and passengers over months

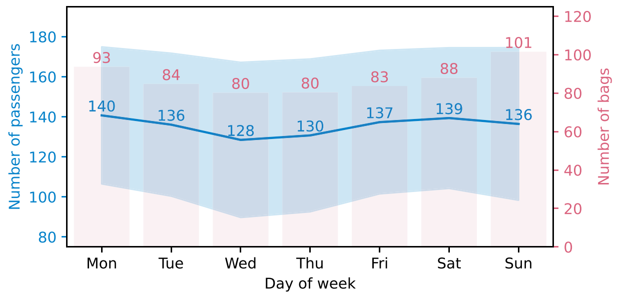

(b) Number of bags and passengers over days

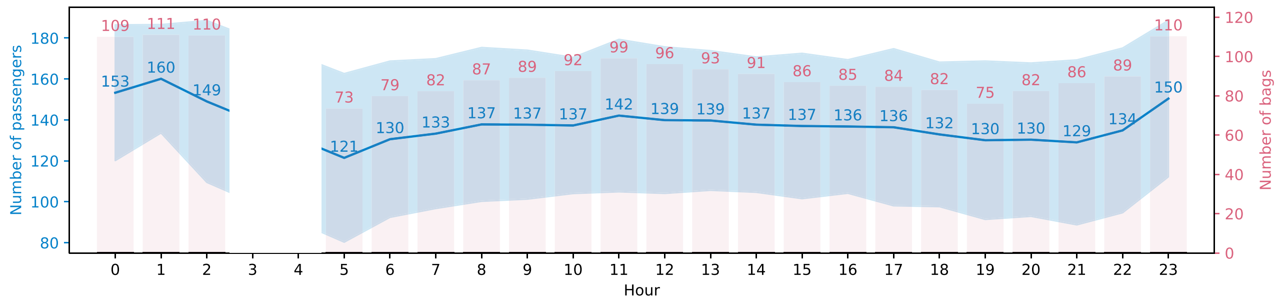

(c) Number of bags and passengers over hours

Figure 7 Passenger and bag counts over time.

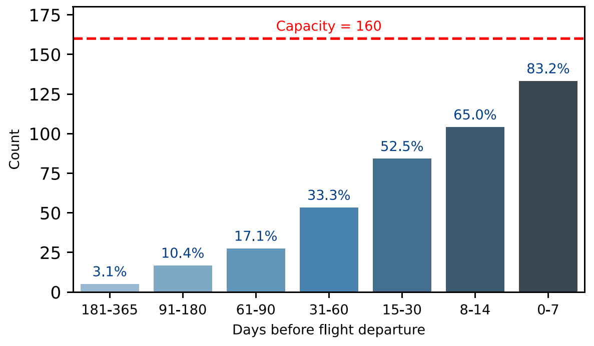

Figure 8 Cumulative number of tickets sold before departure (Hub1 to New York).

In Equation (3), the subscript '+' in $(\hat{y}_i - y_i)_+$ means only the positive part of $(\hat{y}_i - y_i)$ is taken. For $\hat{y}_i < y_i$, 0 is used. c_o and c_u are the overestimation and underestimation cost coefficients, respectively. When c_o and c_u are assigned different values, overestimation and underestimation are penalized differently. The c_u to c_o ratio depends on how likely it is that the space or weight allowance for checked baggage is exceeded for a flight. When the likelihood is relatively low, the coefficient for underestimation c_u should be relatively low while still being greater than c_o. When the checked baggage allowance is frequently exceeded, c_u should be significantly larger than c_o. As this likelihood varies over time and with flights, an airline should carefully determine the c_u to c_o ratio to be consistent with their own operations.

4.2 Simple benchmark: multiple linear regression

We first consider an MLR model that assumes a linear relation between features $\mathbf{x}$ and the main response y. As MLR has been studied rigorously for many decades, it has been applied in many practical contexts of business and engineering. The major reason for considering this is to explore the simplest possibility that gives the smallest risk of model overfitting. Another benefit of MLR lies in its interpretability. The estimated linear coefficients are straightforward to interpret as the main effects of exploratory variables. An MLR model is formally described as

$$f(\mathbf{x}) = \boldsymbol{a}^{\mathrm{T}}\mathbf{x} + b, \tag{4}$$

where $\boldsymbol{a}$ and b are the model parameters.

In this study, the asymmetric loss function $J(\hat{f})$ for MLR model can be expressed as

$$\text{Minimize}_{\boldsymbol{a},b}\, J(\hat{f}) = \sum_{i=1}^{N} \frac{c_o}{2}(\boldsymbol{a}^{\mathrm{T}}\mathbf{x_i} + b - y_i)_+^2 + \frac{c_u}{2}(y_i - \boldsymbol{a}^{\mathrm{T}}\mathbf{x_i} - b)_+^2. \tag{5}$$

To minimize this cost function, gradient descent is used. The gradient descent algorithm is an iterative optimization algorithm that works by starting with an initial set of regression coefficients, $\boldsymbol{a}$ and b, and iteratively updating them in the direction of the steepest descent of the cost function, which is given by the negative gradient of the cost function,

$$\begin{aligned} \boldsymbol{a} &= \boldsymbol{a} - \eta \cdot \nabla_{\boldsymbol{a}} J(\hat{f}) \\ b &= b - \eta \cdot \nabla_b J(\hat{f}), \end{aligned} \tag{6}$$

where η is the learning rate, which controls the step size of the update. Specifically, we can derive the partial derivatives of the loss function with respect to the parameters $\boldsymbol{a}$ and b as follows:

$$\nabla_{\boldsymbol{a}} J(\hat{f}) = \frac{\partial J(\hat{f})}{\partial \boldsymbol{a}} = \frac{1}{N}\sum_{i=1}^{N}\left\{c_o(\boldsymbol{a}^{\mathrm{T}}\mathbf{x_i} + b - y_i)_+ - c_u(y_i - \boldsymbol{a}^{\mathrm{T}}\mathbf{x_i} - b)_+\right\} x_i; \tag{7}$$

$$\nabla_b J(\hat{f}) = \frac{\partial J(\hat{f})}{\partial b} = \frac{1}{N}\sum_{i=1}^{N} c_o(\boldsymbol{a}^{\mathrm{T}}\mathbf{x_i} + b - y_i)_+ - c_u(y_i - \boldsymbol{a}^{\mathrm{T}}\mathbf{x_i} - b)_+. \tag{8}$$

The procedure continues until the cost function converges to a minimum, i.e., until the norm of the gradient becomes sufficiently small or until a maximum number of iterations is reached. As a result, a set of regression coefficients that best match the data is provided by the gradient descent process.

4.3 Proposed approach with extreme gradient boosting

We also consider extreme gradient boosting (XGBoost). It is a variant of gradient boosted decision trees (GBDT; Chen & Guestrin 2016). Like GBDT, its underlying model is an ensemble of decision trees (DTs),

$$f(\mathbf{x}) = \sum_{m=1}^{M} f_m(\mathbf{x}),$$

where $f_m(\mathbf{x})$ represents the mth DT model, and M is the number of DTs in the ensemble. The M DTs are learned sequentially, and the mth DT model f_m is learned at the mth stage of sequential learning. For the first stage, the first decision tree f_1 is fitted to the original training data $\{(\mathbf{x}_i, y_i), i = 1, \ldots, N\}$. For the mth stage, the mth DT f_m is fitted to the residual from the $(m-1)$th stage. Let $\hat{y}_i^{(m-1)} = \sum_{\ell=1}^{m-1} f_\ell(\mathbf{x}_i)$ represent the fit obtained up to the $(m-1)$th stage. DT f_m is fitted to $\{(\mathbf{x}_i, y_i - \hat{y}_i^{(m-1)})\}$. Such sequential stacking of multiple DTs can be easily overfitted. To avoid overfitting, XGBoost applies a model regularization. Specifically, the mth iteration of XGBoost fits f_m to the residual $y_i - \hat{y}_i^{(m-1)}$ by minimizing the following objective function,

$$L^{(m)} = \sum_{i=1}^{N} \ell\left(y_i - \hat{y}_i^{(m-1)}, f_m(\mathbf{x}_i)\right) + \Omega(f_m), \tag{9}$$

where l is a differentiable convex loss function, which is typically a negative log-likelihood for classification problems or the mean squared error for regression problems. The regularization term $\Omega(f_m)$ that penalizes the complexity of the mth tree is defined as

$$\Omega(f_m) = \gamma J_m + \frac{1}{2}\lambda \sum_{j=1}^{J_m} w_j^2, \tag{10}$$

where J_m is the number of leaves in DT f_m, w_j is the complexity score of the jth leaf, and constants γ and λ determine weights on the two terms in the regularization term. For computational feasibility, Chen & Guestrin (2016) developed a second-order approximation to the objective function Equation (9) as

$$L^{(m)} \simeq \sum_{i=1}^{N} \left[\ell(y_i, \hat{y}^{(m-1)}) + g_i f_m(\mathbf{x}_i) + \frac{1}{2} h_i f_m^2(\mathbf{x}_i) \right] + \Omega(f_m), \tag{11}$$

where $g_i = \partial_{\hat{y}^{(m-1)}} l(y_i, \hat{y}^{(m-1)})$ and $h_i = \partial^2_{\hat{y}^{(m-1)}} l(y_i, \hat{y}^{(m-1)})$ are first- and second-order gradients of the loss function $l(y_i, \hat{y}^{(m-1)})$. We derive the derivatives for the asymmetric loss function:

$$g_i = \sum_{i=1}^{N} c_o(\hat{y}_i - y_i)_+ - c_u(y_i - \hat{y}_i)_+; \tag{12}$$

$$h_i = \sum_{i=1}^{N} c_o(\hat{y}_i - y_i)_+^0 - c_u(y_i - \hat{y}_i)_+^0. \tag{13}$$

After removing the constant terms in Equation (11) and expanding $\Omega(f_m)$, the objective function is written as

$$\begin{aligned} \tilde{L}^{(m)} &= \sum_{i=1}^{N} \left[g_i f_m(\mathbf{x}_i) + \frac{1}{2} h_i f_t^2(\mathbf{x}_i) \right] + \gamma J_m + \frac{1}{2}\lambda \sum_{j=1}^{J_m} w_j^2 \\ &= \sum_{j=1}^{J_m} \left[\Big(\sum_{i\in I_j} g_i\Big) w_j + \frac{1}{2}\Big(\sum_{i\in I_j} h_i + \lambda\Big) w_j^2 \right] + \gamma J_m, \end{aligned} \tag{14}$$

where $I_j = \{i \mid q(\mathbf{x}_i) = j\}$ is the data samples in leaf j. After creating the second-order approximation of the objective function, XGBoost proceeds to build the model by adding trees to the ensemble. At each iteration, the algorithm calculates the leaf weights that minimize the objective function for the newly added tree. This process of adding trees continues until a stopping criterion is satisfied, which is often determined by the validation error. This criterion prevents overfitting of the model and ensures that the algorithm can generalize well to unseen data.

4.4 Proposed approach with light gradient boosting machine

Another approach we consider is the light gradient boosting machine (LightGBM), an efficient and scalable implementation of gradient boosting framework (Ke et al., 2017). LightGBM is known for its high efficiency, low memory usage, and its ability to handle large-scale data. The core algorithm is similar to that of XGBoost, but with some distinct features that enhance performance, particularly on large datasets.

LightGBM builds the model in the form of an ensemble of decision trees, similar to XGBoost,

$$f(\mathbf{x}) = \sum_{m=1}^{M} f_m(\mathbf{x}), \tag{15}$$

where $f_m(\mathbf{x})$ represents the mth decision tree model, and M is the total number of trees.

Two unique features of LightGBM are its gradient-based one-side sampling (GOSS) and exclusive feature bundling (EFB), which reduce the amount of data and number of features without significant loss of accuracy. The GOSS method focuses on instances with larger gradients, as they are considered more informative, while EFB effectively reduces the number of features by bundling mutually exclusive features.

The training process involves minimizing a similar objective function as XGBoost, with a loss function and a regularization term. However, LightGBM uses histogram-based algorithms for computing the gradients, which significantly speeds up the learning process. The objective function is defined as

$$L = \sum_{i=1}^{N} \ell(y_i, \hat{y}_i) + \Omega(f), \tag{16}$$

where $\ell(y_i, \hat{y}_i)$ is the loss function, $\hat{y}_i$ is the predicted value, and $\Omega(f)$ is the regularization term.

The loss function can be tailored to our specific problem, considering the asymmetric cost of underestimation and overestimation as previously described. The regularization term helps to control the complexity of the model and prevent overfitting. The algorithm iteratively builds trees, each focusing on correcting the errors of the previous ensemble.

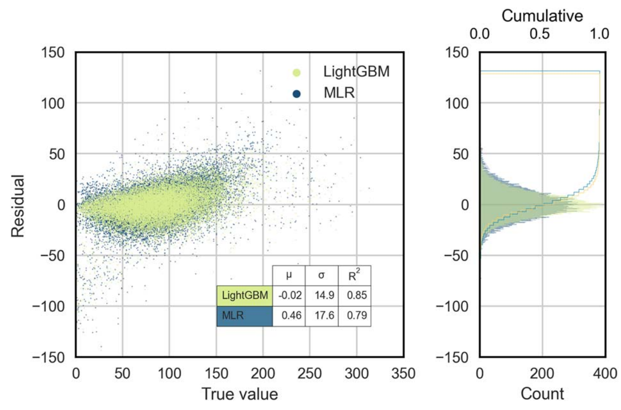

	μ	σ	R^2
LightGBM	-0.02	14.9	0.85
MLR	0.46	17.6	0.79

Figure 9 Histograms for residuals under symmetric loss.

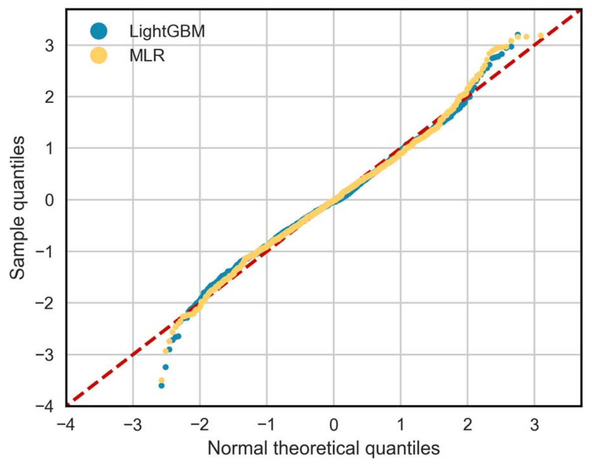

Figure 10 Quantiles of residuals of MLR and LightGBM.

To optimize the LightGBM model, we employ a similar gradient descent strategy as described for the MLR model, with the objective of minimizing the asymmetric loss function. The LightGBM framework offers several hyperparameters such as the number of leaves, the learning rate, and the maximum depth of trees, which we can tune to achieve the best model performance.

In summary, LightGBM offers an efficient and effective approach for predictive modeling in large-scale data scenarios. Its ability to handle large datasets with a high speed and lower memory consumption, while providing high accuracy, makes it a suitable choice for our predictive analysis of checked baggage volume.

5. Results

5.1 Comparison of MLR and LightGBM under symmetric loss

We first compare MLR and LightGBM without considering an asymmetric loss function. In other words, we assume $c_u = c_o = 1$ in this section. A standard hold-out testing method is adopted where 75 per cent of the samples (541,917 samples) are in the training dataset and the remaining 180,639 samples are in the testing dataset. Figure 9 compares the residual distributions for MLR and LightGBM. In Fig. 9, the mean residuals for LightGBM and MLR are virtually the same and close to 0. The standard deviation of MLR is 17.6, which is greater than 14.9 for LightGBM. This is consistent with the finding that the R^2 value achieved with MLR (0.79) is clearly lower than that of LightGBM (0.85). The scatter plot in Fig. 9 shows that the residuals for MLR are more dispersed than those for LightGBM, a further sign of weaker prediction performance. While a considerable number of residuals are outside of the range $[-30, 30]$ for MLR, significantly more LightGBM residuals are within the range. For MLR, when the true bag count is below 100, residuals tend to be negative (i.e., underprediction); when the true bag count is over 100, residuals tend to be positive (i.e., overprediction). For LightGBM, the correlation of residuals and true values is lower. Note that the residuals from only 1 per cent of all the testing samples are shown in Fig. 9 to avoid overcrowding.

With 0.5 per cent of testing samples drawn, the quantile–quantile plot in Figure 10 indicates that the residuals of LightGBM and MLR largely follow a normal distribution, as most of the points fall approximately on the 45-degree reference line. This further indicates that MLR captures the underlying relation between various features and the target variable quite well.

The above comparisons suggest that the advanced LightGBM outperforms the standard linear regression model. LightGBM has multiple advantages over MLR. First, LightGBM, being a tree-based method, can naturally model these non-linear relationships, making it more effective for complex datasets. Second, LightGBM automatically captures interactions between features through its hierarchical tree structure. Lastly, LightGBM is more robust to outliers as decision trees split the data based on certain conditions, reducing the influence of extreme values.

We further note that for both methods, if the true value is smaller than 50 or larger than 200, it is quite challenging to predict the true value accurately, as shown in Fig. 9. The primary reason is that there are no adequate training data in those bag count ranges to understand the relation between the bag count and other features as stated earlier. For instance, wide-body aircraft, which can accommodate more than 200 passengers, are severely under-represented (accounting for only 1.85 per cent of samples), as shown in Fig. 4.

5.2 Comparison of three methods under asymmetric loss

We next compare the three methods when an asymmetric loss function is considered. We use the same hold-out testing method described in Section 5.1. To model the degree of asymmetry, we set c_o to be 1 while considering four values for c_u: 1, 5, 10, and 15. When $c_u = c_o$, the asymmetric loss function reduces to a symmetric one. As the value of c_u increases, the penalty for underestimation grows. The XGBoost hyperparameters are tuned by Bayesian optimization (Snoek et al., 2012). The hyperparameter tuning process has 100 iterations. A hold-out strategy is used that aims to minimize the sum of asymmetric loss function values over testing samples. After hyperparameter tuning, values of some key hyperparameters of XGBoost are: learning rate = 0.1, maximum tree depth = 6, minimum sum of instance weight (hessian) needed in a child = 19, and subsample ratio = 0.8. While using more estimators leads to better performances, the number of estimators is configured as 600 because no significant improvements are observed by increasing this value. As the XGBoost API supports multi-threading, the number of threads is configured as the maximum value, namely 16. Similar to XGBoost, the hyperparameters for LightGBM are also tuned using Bayesian optimization. Key LightGBM hyperparameters include a learning rate of 0.1, a maximum depth of 6, and 31 leaves per tree, which is a default yet effective choice for LightGBM. The number of estimators is kept the same as XGBoost at 600. The subsample ratio is set at 0.8, aligning with the XGBoost set-up. The LightGBM

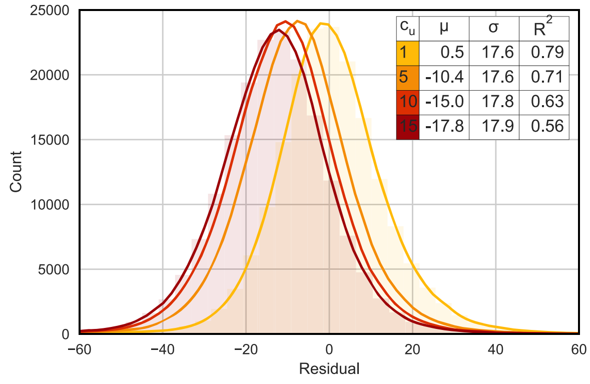

c_u	μ	σ	R^2
1	0.5	17.6	0.79
5	-10.4	17.6	0.71
10	-15.0	17.8	0.63
15	-17.8	17.9	0.56

Figure 11 Effect of c_u on MLR residual distribution.

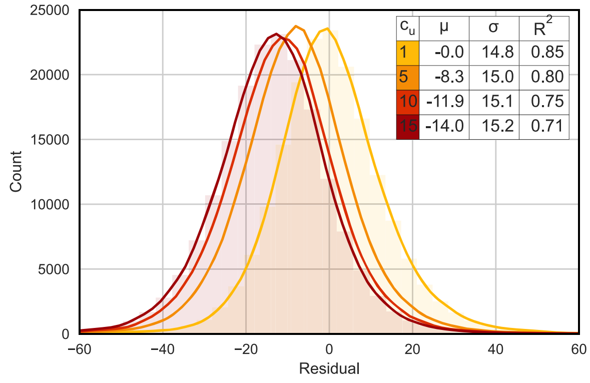

c_u	μ	σ	R^2
1	-0.0	14.8	0.85
5	-8.3	15.0	0.80
10	-11.9	15.1	0.75
15	-14.0	15.2	0.71

Figure 12 Effect of c_u on LightGBM residual distribution.

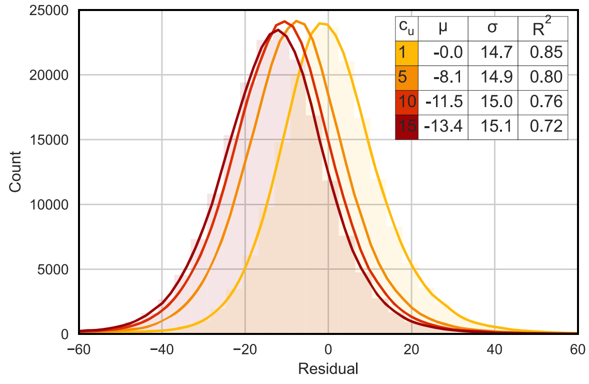

c_u	μ	σ	R^2
1	-0.0	14.7	0.85
5	-8.1	14.9	0.80
10	-11.5	15.0	0.76
15	-13.4	15.1	0.72

Figure 13 Effect of c_u on XGBoost residual distribution.

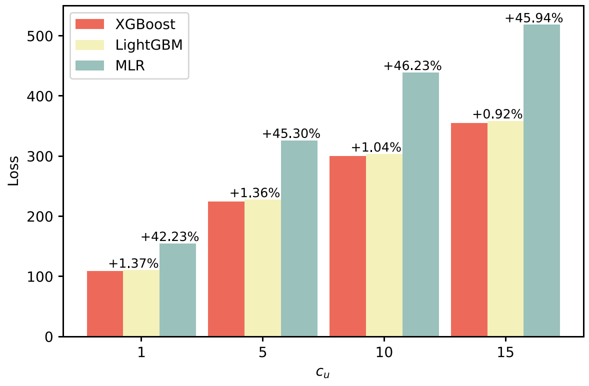

Figure 14 Comparison of loss function values under different c_u.

model is configured to use all available cores to ensure efficient computation.

Figures 11, 12, and 13 compare the residual distributions of MLR, LightGBM, and XGBoost, respectively. Clearly, the distributions of XGBoost and LightGBM are tighter than MLR. The standard deviations of the residuals of XGBoost and LightGBM are around 15 while MLR yields a larger standard deviation of 17.6 when $c_u = 1$. This means that XGBoost and LightGBM outperform MLR when a symmetric loss function is considered. As c_u increases from 1 to 10, the distribution of residuals shifts to the left and the standard deviation of residuals increases, for all three methods. As c_u increases further to 15, the change in the mean and standard deviation of residuals becomes relatively small. This means that the impact of a growing c_u on the residual distribution diminishes. While c_u increases from 1 to 15, XGBoost and LightGBM have a consistently better predictive performance than MLR judged by the distribution of residuals. When c_u increases from 1 to 15, the R^2 of MLR decreases from 0.79 to 0.56; LightGBM is capable of achieving a high R^2 consistently, although it decreases from 0.85 to 0.71; XGBoost performs similar to LightGBM, with R^2 of 0.85 to 0.72.

We briefly show why R^2 decreases as coefficient c_u in the asymmetric loss function increases. The coefficient of determination (i.e., R^2) is defined as

$$R^2 = 1 - \frac{\sum_i (y_i - \hat{y}_i)^2}{\sum_i (y_i - \bar{y}_i)^2}. \tag{17}$$

R^2 can be rewritten as

$$R^2 = 1 - \frac{\text{MSE}}{\text{Var(Y)}} \tag{18}$$

by noting the definitions of mean squared error (MSE) and variance $\text{MSE} = \sum_i (y_i - \hat{y}_i)^2$ and $\text{Var(Y)} = \sum_i (y_i - \bar{y}_i)^2$.

As the variance of the target variable is a constant, it is clear that R^2 is a standardized or rescaled MSE. In particular, a larger MSE leads to a smaller R^2. As an asymmetric loss function is adopted in training the learning algorithm, the asymmetric loss is the optimization objective, rather than MSE (a symmetric metric). In the special case where $c_u = 1$, asymmetric loss reduces to symmetric loss, which means minimizing an asymmetric loss gives the minimal MSE, and thus the highest R^2. As c_u increases, underestimation is more heavily penalized than overestimation, which means the predictive algorithm will overestimate, thus directly hurting MSE (becoming larger) and R^2 (becoming smaller). Figures 11, 12, and 13 also show how R^2 varies with c_u for the three methods.

Figure 14 compares the loss function values of three methods, which shows that MLR consistently has the highest loss for all values of c_u, and XGBoost performs with the lowest loss, indicating that XGBoost outperforms LightGBM and MLR. Furthermore, as c_u increases from 1 to 15, the loss values for all methods increase, with MLR exhibiting a percentage increase in loss of about 45 per cent compared to XGBoost. Overall, XGBoost outperforms LightGBM very slightly and MLR by a notable margin when an asymmetric loss function is considered, regardless of the value of c_u.

5.3 Exploration on residuals of XGBoost

Here we explore the predictive performance of XGBoost across different categories when $c_o = 1$ and $c_u = 5$. For instance, we seek to explore whether XGBoost would achieve similar performance for flights on different days of the week. Figure 15 thus shows the 25th percentile, median, and 75th percentile of the loss function

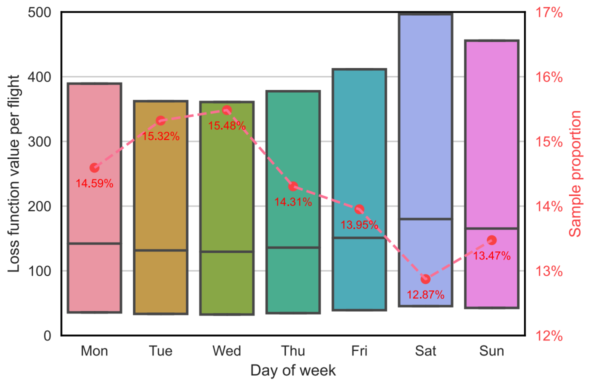

Figure 15 Loss function value per flight of XGBoost by day of the week.

value. No significant differences are observed over different days of the week except for Saturday with a higher loss function value. This means that the performance of XGBoost is overall consistent over the days.

We next define a criterion for misprediction. We state a value is mispredicted, thus constituting a misprediction, if the absolute residual is larger than 25 (i.e., $| \; y - \hat{y} \; | > \; 25$) and the relative deviation is larger than 20 per cent (i.e., $| \; y - \hat{y} \; | \; /y > 20$ per cent). Then for each destination city, we can compute the proportion for mispredicted samples. Figure 16 shows the top destination cities with the highest misprediction proportions. The two notable destinations are Anchorage, Alaska and Hayden, Colorado. Figure 17 shows that the residual distribution for Atlanta, Georgia is clearly tighter than those for the two identified airports with significant mispredictions.

One possible reason for baggage mispredictions for Anchorage-bound flights is that 75 out of 268 flights (28.0 per cent) arriving in Anchorage are operated by wide-body aircraft. The number of bags per flight for Anchorage is 178 on average while the average bag count for the whole dataset is 92. The latter city, Hayden, Colorado, is one of the smallest cities that has air services in the US because its population was only around 2,000 in 2020. The whole dataset has only 126 samples for Hayden, covering a four-month winter period from December to March. In other words, those are seasonable flights. It is very likely that most of those passengers are taking ski vacations in Hayden during winter months. It is thus understandable that those passenger characteristics are quite different. For instance, on average 108 passengers are classified as leisure travelers and 8 passengers are classified as business travelers by Airline λ (i.e., the percentage for business travelers is 0.7 per cent). In contrast, a much higher proportion of passengers (i.e., 33 per cent) travel for business instead of leisure, as classified by Airline λ. In addition, a higher percentage of passengers travel with a child or infant on Hayden-bound flights than the same percentage for the entire dataset. Clearly, the underlying patterns for the identified cities in Fig. 16 are different from most other flights in the dataset, which means that those associated flights can be considered 'outliers'. Therefore, substantial mispredictions occur.

Figure 18 shows the misprediction proportion for each fleet type. Four leading fleet types with a large misprediction proportion are all wide-body aircraft, which suffer from the same under-representation issue. Figure 19 also shows that the residual distribution for Airbus A319 is much tighter than the distributions for Boeing 777 and 787.

Even though XGBoost achieves a very high prediction accuracy overall, its performance may not be satisfactory for certain flights with insufficient data support. For instance, mispredictions are significant for those flights associated with the identified destination cities and fleet types. Additional efforts need to be made to improve the predictive performance of those outlier flights. For instance, more historical data, covering multiple years rather than one, are necessary to achieve an acceptable prediction performance.

6. Discussion

Selecting an appropriate prediction algorithm is never an easy task as a trade-off between a learning algorithm's complexity and its performance needs to be made. For checked baggage prediction, the historical average approach is used in practice primarily due to its intuitiveness and simplicity. However, even a very typical linear regression algorithm can outperform the state-of-the-practice approach by a good margin; an advanced machine learning algorithm, such as LightGBM or XGBoost, is more effective in achieving high prediction accuracy, which is expected. Despite the superior performance of LightGBM and XGBoost, especially measured by accuracy, both gradient boosting methods, as an ensemble model, are not interpretable

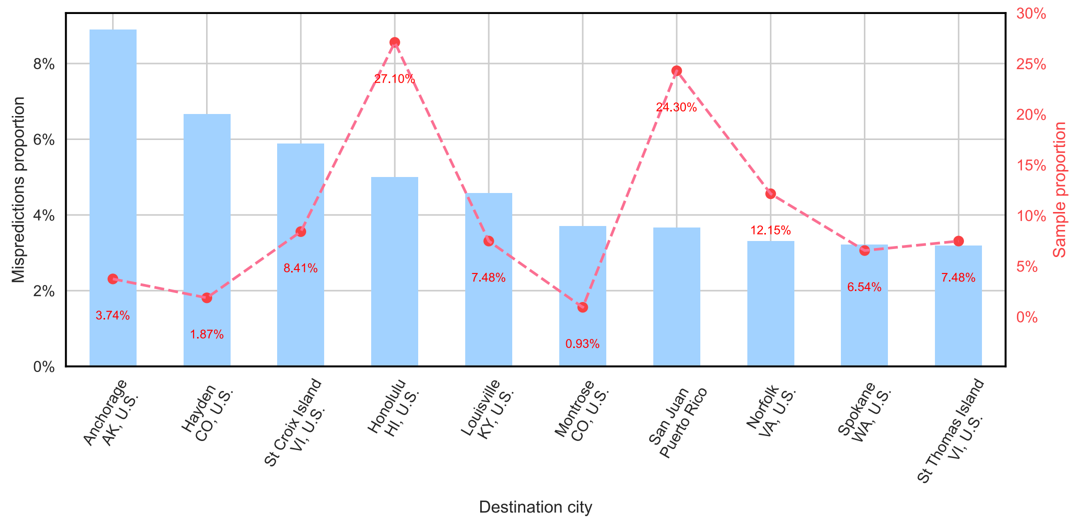

Figure 16 Distribution of top 10 destination cities with significant mispredictions.

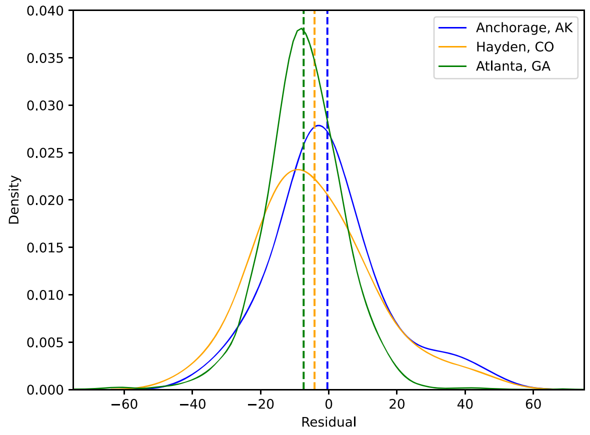

Figure 17 Residual distributions for three example destination cities.

(Luo et al., 2022; Shi et al., 2023). It is less transparent than the linear regression or historical average approach for analysts to understand how a value is predicted. From a pragmatic perspective, low interpretability means a lower chance of acceptance by analysts. In addition, the complexity of XGBoost is high, as it requires more hyperparameter tuning than MLR. Figure 20 clearly indicates that the MLR training time is almost negligible in relative to the training time for XGBoost even though 16 threads are used in parallel to train XGBoost. LightGBM, while it is also a gradient boosting method, takes 11.4 and 28.2 seconds for training with 100,000 and 700,000 samples, respectively, which are dramatically shorter than for XGBoost.

For this specific prediction task, the relation between the target variable (i.e., the checked bag count) and a few key features (e.g., the revenue passenger count) is found to be largely linear, although other factors (e.g., destination city characteristics and travel seasons) also play a role. The clear linear relation explains why a linear regression algorithm can achieve a satisfactory performance. Linear regression results are highly interpretable. For instance, the coefficient for the number of passengers in the main cabin measures how many bags a passenger in the main cabin carries. Although this coefficient varies over time and across regions, values of this coefficient can be tracked by airlines to understand the trends in checked baggage. Linear regression is thus recommended for replacing the historical average approach. XGBoost or other complex learning algorithms are recommended for those cases where the linear relation is unclear or not well characterized by available data.

A more detailed baggage prediction model can be developed at the individual passenger level, as the current analysis is conducted at the flight level. In the individual prediction model, historical baggage data for an individual can be leveraged to understand how likely they are to check bags. Then, individual bag counts can be aggregated to obtain the flight-level bag count.

7. Conclusions

With a very large-scale multi-source dataset covering the entire USA, we customized three machine learning algorithms of various complexities to predict the number of checked bags on a flight and evaluated the performance improvements of those three machine learning algorithms. Our primary contribution is to systematically consider the different impacts of overprediction and underprediction on airline operations and to customize three machine learning algorithms with a piecewise quadratic loss function. Our numerical experiments indicate that: (1) the two gradient boosting methods can significantly outperform standard MLR; (2) XGBoost can further improve the predictive performance of LightGBM, regardless of whether the asymmetric loss function is considered or not; (3) LightGBM is more efficient than XGBoost in terms of training process. We also find that even though XGBoost has remarkably high accuracy in predicting the bag count at the flight level, the performance is not uniform, as checked bags in certain categories cannot be predicted satisfactorily. For instance, the misprediction portion tends to be high for flights to Anchorage, Alaska, or flights operated by wide-body aircraft. One major shortcoming of XGBoost is its low interpretability. Therefore, it is noted that an ideal prediction algorithm for adoption in practice should strike a reasonable balance between accuracy and interpretability.

This present study can be improved in the following ways. First, the entire dataset can be partitioned so that certain categories of samples (e.g., those involving wide-body aircraft) can be predicted by dedicated machine learning algorithms with high complexity while the rest of the samples can be predicted with a low-complexity algorithm. Second, the checked baggage weight can be further predicted when such data are available. Third, additional passenger-related features, such as gender, age, and travel duration (time difference between departure and arrival times), may be added to improve the predictive performance. Additionally, efforts are needed to investigate how such a prediction tool can be incorporated into airline revenue management. Finally, in this study, the baggage prediction is conducted only

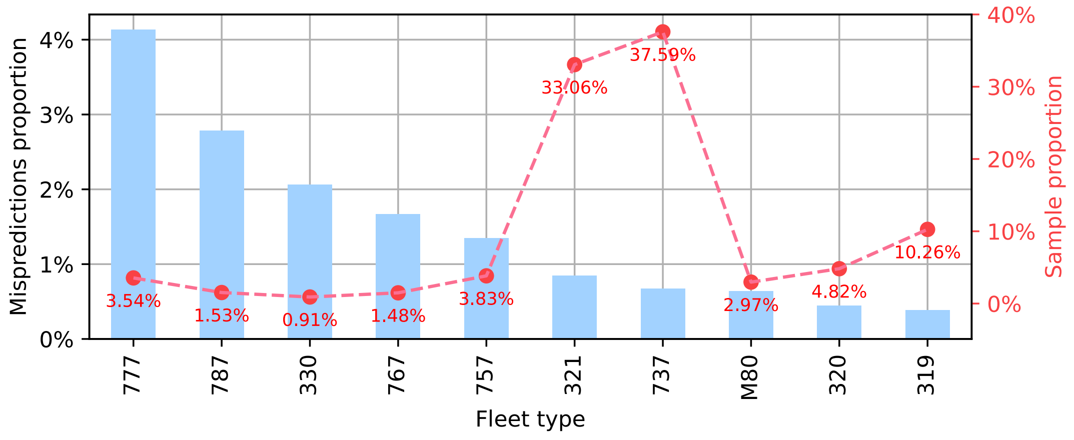

Figure 18 Distribution of fleet types with significant mispredictions.

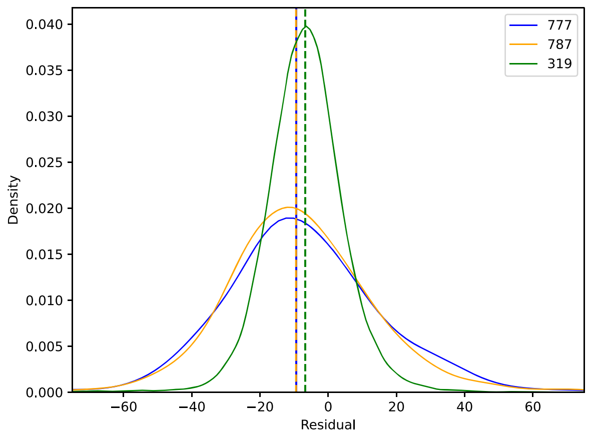

Figure 19 Residual distributions for three example fleet types.

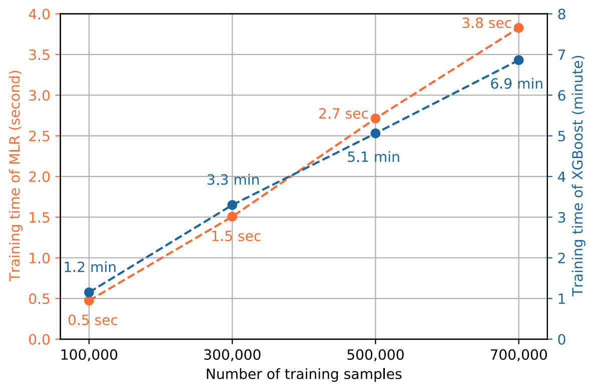

Figure 20 Training time as a function of training sample size.

once, several hours prior to departure. The predicted baggage volume, when available, initializes the aircraft load planning process. As the availability of information varies over time, it is interesting and relevant to update prediction results when new information (e.g., trip cancellations or itinerary changes) becomes available as a flight's departure nears. The current static prediction can be extended to a dynamic prediction in a future study.

Acknowledgments

The corresponding author is partially supported by the National Science Foundation (Grant Nos 2055347, 2100745, and 2332161). The data support from Airline λ is appreciated.

Author contributions

Shijie Chen (Methodology, Investigation, Software, Writing—original draft, Writing—review & editing), Chiwoo Park (Methodology, Validation, Writing—original draft), Qianwen Guo (Investigation, Validation, Writing—original draft), Yanshuo Sun (Conceptualization, Supervision, Validation, Writing—original draft, writing—review & editing). All authors reviewed the manuscript.

Conflict of interest statement

The corresponding author is an Editorial Board Member for *Intelligent Transportation Infrastructure* and is blinded from reviewing or making decisions about the manuscript. The authors do not have any competing financial interests to declare.

References

Barua, L., Zou, B., and Zhou, Y. (2020) 'Machine Learning for International Freight Transportation Management: A Comprehensive Review', *Research in Transportation Business & Management*, **34**: 100453. https://doi.org/10.1016/j.rtbm.2020.100453.

BEONTRA (2022) '*Machine Learning Helps Improve Baggage Handling Planning*', blog, https://www.beontra.com/machine-learning-helps-improve-baggage-handling-planning/ accessed 23 July 2023.

Brandt, F. and Nickel, S. (2019) 'The Air Cargo Load Planning Problem–A Consolidated Problem Definition and Literature Review on Related Problems', *European Journal of Operational Research*, **275**: 399–410. https://doi.org/10.1016/j.ejor.2018.07.013.

Chen, T. and Guestrin, C. (2016) 'XGboost: A Scalable Tree Boosting System', in *Proceedings of the 22nd ACM SIGKDD Conference on Knowledge Discovery and Data Mining*, pp. 785–94. New York: Association for Computing Machinery.

Cheng, S., Gao, Q., and Zhang, Y. (2014) 'Comparative Study on Forecasting Method of Departure Flight Baggage Demand', in *Proceedings of 2014 IEEE Chinese Guidance, Navigation and Control Conference*, pp. 1600–5. Piscataway, NJ: IEEE.

Chung, S-H. et al. (2020) 'Data Science and Analytics in Aviation', *Transportation Research Part E: Logistics and Transportation Review*, **134**: 101837. https://doi.org/10.1016/j.tre.2020.101837.

FAA (2024) '*Next Generation Air Transportation System (NextGen)*', https://www.faa.gov/nextgen accessed 16 April 2024.

FAA (2023). Chapter 10: Weight and Balance, *Pilot's Handbook of Aeronautical Knowledge*, https://www.faa.gov/sites/faa.gov/files/12_phak_ch10.pdf accessed 23 July 2023.

FAA (2016). *Weight & Balance Handbook*, https://www.faa.gov/sites/faa.gov/files/regulations_policies/handbooks_manuals/aviation/FAA-H-8083-1.pdf accessed 23 July 2023.

FAA (2022) 'Passenger Boarding (Enplanement) and All-Cargo Data for U.S. Airports', https://www.faa.gov/airports/planning_capacity/passenger_allcargo_stats/passenger.

Gallego, C. E. V. et al. (2019) 'A Machine Learning Approach to Air Traffic Interdependency Modelling and its Application to Trajectory Prediction', *Transportation Research Part C: Emerging Technologies*, **107**: 356–86. https://doi.org/10.1016/j.trc.2019.08.015.

Hanumantha, G. J. et al. (2020) 'Demand Prediction and Dynamic Workforce Allocation to Improve Airport Screening Operations', *IISE Transactions*, **52**: 1324–42. https://doi.org/10.1080/24725854.2020.1749765.

Jardines, A., Soler, M., and García-Heras, J. (2021) 'Estimating Entry Counts and ATFM Regulations during Adverse Weather Conditions Using Machine Learning', *Journal of Air Transport Management*, **95**: 102109. https://doi.org/10.1016/j.jairtraman.2021.102109.

Ke, G. et al. (2017) 'LightGBM: A Highly Efficient Gradient Boosting Decision Tree', *Advances in Neural Information Processing Systems*, **30**: 3149–57.

Khan, W. A. et al. (2021) 'Hierarchical Integrated Machine Learning Model for Predicting Flight Departure Delays and Duration in Series', *Transportation Research Part C: Emerging Technologies*, **129**: 103225. https://doi.org/10.1016/j.trc.2021.103225.

Luo, Z. et al. (2022) 'Research on Influencing Factors of Asphalt Pavement International Roughness Index (IRI) Based on Ensemble Learning', *Intelligent Transportation Infrastructure*, **1**: liac014. https://doi.org/10.1093/iti/liac014.

Ma, Q. et al. (2021) 'Research on Prediction of Checked-Baggage Departed from Airport Terminal Based on Time Series Analysis', in *Proceedings of the 7th Annual International Conference on Network* *and Information Systems for Computers (ICNISC)*, pp. 264–9. Piscataway, NJ: IEEE.

Mikram, M. et al. (2020) 'Unit Load Devices (ULD) Demand Forecasting in the Air Cargo for Optimal Cost Management', *Journal of Automation Mobile Robotics and Intelligent Systems*, **14**: 71–80. https://doi.org/10.14313/JAMRIS/3-2020/37.

Mondoloni, S. and Rozen, N. (2020) 'Aircraft Trajectory Prediction and Synchronization for Air Traffic Management Applications', *Progress in Aerospace Sciences*, **119**: 100640. https://doi.org/10.1016/j.paerosci.2020.100640.

Rodríguez-Sanz, Á. et al. (2019) 'Assessment of Airport Arrival Congestion and Delay: Prediction and Reliability', *Transportation Research Part C: Emerging Technologies*, **98**: 255–83. https://doi.org/10.1016/j.trc.2018.11.015.

Shi, C. et al. (2023) 'A BIM-Based Framework for Automatic Numerical Modelling and Geotechnical Analysis of a Large-Scale Deep Excavation for Transportation Infrastructures', *Intelligent Transportation Infrastructure*, **2**: liad012. https://doi.org/10.1093/iti/liad012.

Snoek, J., Larochelle, H., and Adams, R. P. (2012) 'Practical Bayesian Optimization of Machine Learning Algorithms', *Advances in Neural Information Processing Systems*, **25**: 2951–9.

Sun, Y. et al. (2018) 'Analyzing High Speed Rail Passengers' Train Choices Based on New Online Booking Data in China', *Transportation Research Part C: Emerging Technologies*, **97**: 96–113. https://doi.org/10.1016/j.trc.2018.10.015.

TSA (2022) *TSA Checkpoint Travel Numbers*, https://www.tsa.gov/coronavirus/passenger-throughput, accessed 23 July 2023.

Tseremoglou, I., Bombelli, A., and Santos, B. F. (2022) 'A Combined Forecasting and Packing Model for Air Cargo Loading: a Risk-Averse Framework', *Transportation Research Part E: Logistics and Transportation Review*, **158**: 102579. https://doi.org/10.1016/j.tre.2021.102579.

US Census Bureau (2021) *City and Town Population Totals: 2010–2020*, https://www.census.gov/programs-surveys/popest/technical-documentation/research/evaluation-estimates/2020-evaluation-estimates/2010s-cities-and-towns-total.html accessed 23 July 2023.

van Leeuwen, H. et al. (2020) 'Lost and Found: Predicting Airline Baggage at-Risk of Being Mishandled', in A. P. Rocha, L. Steels, and J. van den Herik (eds), *Proceedings of the 12th International Conference on Agents and Artificial Intelligence (ICAART), Volume 2*, pp. 172–81. Berlin: Springer.

Wang, Z., Liang, M., and Delahaye, D. (2020) 'Automated Data-Driven Prediction on Aircraft Estimated Time of Arrival', *Journal of Air Transport Management*, **88**: 101840. https://doi.org/10.1016/j.jairtraman.2020.101840.

Wold, S. et al. (1984) 'The Collinearity Problem in Linear Regression. The Partial Least Squares (PLS) Approach to Generalized Inverses', *SIAM Journal on Scientific and Statistical Computing*, **5**: 735–43. https://doi.org/10.1137/0905052.

Wu, X. et al. (2022) 'Long-Term 4D Trajectory Prediction Using Generative Adversarial Networks', *Transportation Research Part C: Emerging Technologies*, **136**: 103554. https://doi.org/10.1016/j.trc.2022.103554.

Xu, S., Chan, H. K., and Zhang, T. (2019) 'Forecasting the Demand of the Aviation Industry Using Hybrid Time Series SARIMA-SVR Approach', *Transportation Research Part E: Logistics and Transportation Review*, **122**: 169–80. https://doi.org/10.1016/j.tre.2018.12.005.

Xu, Y., Wandelt, S., and Sun, X. (2024) 'Airline Scheduling Optimization: Literature Review and a Discussion of Modeling Methodologies', *Intelligent Transportation Infrastructure*, **3**: liad026. https://doi.org/10.1093/iti/liad026.

Appendix A. A List of considered features

Table A1 lists the name, description, and variable type of each feature that is considered in the case study.

Table A1. Descriptions and variable types of features

Feature name	Description [# features if categorical]	Variable type
Flight-related		
FLIGHT_DEP_M	Scheduled departure date (month only) [12]	Categorical
FLIGHT_ARVL_M	Scheduled arrival date (month only) [12]	Categorical
FLIGHT_DEP_DW	Scheduled departure date (day of the week) [7]	Categorical
FLIGHT_ARVL_DW	Scheduled arrival date (day of the week) [7]	Categorical
FLIGHT_DEP_HOUR	Scheduled departure time (hour only) [24]	Categorical
FLIGHT_ARVL_HOUR	Scheduled arrival time (hour only) [24]	Categorical
LEG_DISTANCE	Number of miles of this leg	Continuous
ORIG_CITY_NM	Origin city name [112]	Categorical
DEST_CITY_NM	Destination city name [116]	Categorical
AIRCRAFT_TYPE	Type of aircraft (wide or narrow body) [2]	Categorical
FLEET_TYPE	Fleet classification code [11]	Categorical
TTL_SEATS	Total number of seats	Continuous
TTL_PAX	Total number of passengers	Continuous
LF	Load factor = number of passengers/number of seats	Continuous
Passenger-related		
PAX_REV	Number of revenue passengers on the flight	Continuous
PAX_NONREV	Number of non-revenue leisure passengers	Continuous
PAX_POS_SPC	Number of non-revenue business passengers	Continuous
PAX_CONNECT	Number of passengers on the flight who have a connection	Continuous
PAX_LOCAL	Number of passengers who start their flight at the departure airport	Continuous
PAX_BUSINES	Number of passengers classified as business passengers	Continuous
PAX_LEISURE	Number of passengers classified as leisure passengers	Continuous
PAX_CHILD_WINF	Number of passengers with a child or infant	Continuous
PAX_ASSIST	Number of passengers who require assistance	Continuous

(Continued)

Table A1. Continued

Feature name	Description [# features if categorical]	Variable type
PAX_ANIMAL	Count of all the service/emotional support animals on the flight	Continuous
LYLTY_X	Number of passengers with a loyalty status of X	Continuous
NUM_GROUP_Y	Number of groups that contain Y passengers	Continuous
CABIN_FIRST	Number of passengers in first class	Continuous
CABIN_BUSINESS	Number of passengers in business class	Continuous
CABIN_PREM	Number of passengers in premium economy	Continuous
CABIN_MAIN	Number of passengers in main cabin	Continuous
BOOK_DAYS2DEP_Z	Number of passengers booked within Z days prior to departure	Continuous
BOTH_CARD	Number of passengers who hold credit cards A and B	Continuous
CARD1	Number of passengers who hold credit card A only	Continuous
CARD2	Number of passengers who hold credit card B only	Continuous
SALES_BUSINESS	Number of passengers booking via a business sales channel	Continuous
SALES_DIRECT	Number of passengers booking via official websites	Continuous
SALES_LEISURE	Number of passengers booking via a leisure sales channel	Continuous
SALES_OTA	Number of passengers booking via an online travel agency	Continuous
SALES_TMC	Number of passengers booking via a travel management company	Continuous
Supplemental		
CK_POINT	TSA checkpoint travel numbers	Continuous
ENP_ORIG	Enplanement of origin airport	Continuous
ENP_DEST	Enplanement of destination airport	Continuous
POP_ORIG	Population of origin city	Continuous
POP_DEST	Population of destination city	Continuous